

of time. The authors, however, set  $i_1$  equal to a time function in (10) and claim that  $i_1$  and  $i_2$  are time functions in their rebuttal.

Whether the curves presented by Perlow and Perlman fit measurements taken on a particular upconverter are not at issue here, only the correctness and validity of the derivations.

*S. M. Perlow and B. S. Perlman<sup>4</sup>*

As we have previously stated, (10) represents the transfer characteristic of the up-converter. As such, it is treated as any other nonlinear characteristic would be. Grayzel believes this to be mathematically inconsistent and leads to incorrect results. It will now be shown that two tones applied to the input may indeed be analyzed in such a manner.

When a two-tone test is used to measure intermodulation distortion, two signals of frequencies  $f_a$  and  $f_b$  are applied to the input. The output contains responses at every sum and difference frequency. The frequencies of interest for intermodulation distortion specifications are those corresponding to  $(m+1)f_a - mf_b$  and  $(m+1)f_b - mf_a$ . This was the notation used in the paper. Equation (10) was expanded in a series and  $i_1$  was replaced by  $\cos \omega_a t$  and then later on by  $\cos \omega_a t + \cos \omega_b t$ , expanded to all odd powers. The validity of this series may be seen quite easily by considering a different means of generating the two tones.

Let the two-tone input signals be separated in frequency by  $2\omega_e$ . Therefore

$$\begin{aligned}\omega_a &= \omega_1 + \omega_e \\ \omega_b &= \omega_1 - \omega_e\end{aligned}$$

and (22) becomes:

$$\begin{aligned}i_{\text{signal}} &= |i| (\cos \omega_a t + \cos \omega_b t) \\ &= |i| [\cos (\omega_1 + \omega_e)t \\ &\quad + \cos (\omega_1 - \omega_e)t] \\ &= 2|i| \cos \omega_e t \cos \omega_1 t.\end{aligned}$$

That is, the two original tones may be replaced by a single DSBSC tone. The magnitude of the input signal is no longer a constant but now becomes  $2|i| \cos \omega_e t$ , where  $\omega_e \ll \omega_s$ . Equation (13) may now be written as

$$\begin{aligned}i_s &= A_0 |i| [i_1 - |A_1 i_1|^2 i_3 + |A_1 i_1|^4 i_5 \\ &\quad - |A_1 i_1|^6 i_7 + \dots]\end{aligned}$$

where

$$i_1 = \cos \omega_e t.$$

The intermodulation frequencies corresponding to  $(m+1)f_a - mf_b$  and  $(m+1)f_b - mf_a$  now become  $f_1 \pm (2m+1)f_e$ . Note that the intermodulation frequencies are harmonically related to the difference in frequency between  $\omega_a$  and  $\omega_b$ .

The second term of the above expansion gives rise to the desired output plus a contribution to the first intermodulation distortion product term of the form  $K \cos (\omega_s + 3\omega_e)t$ , or if  $\omega_a$  and  $\omega_b$  are used,  $K \cos (2\omega_a - \omega_b)t$ . The coefficients of this expansion are exactly the same as the coefficients of the expansion in the paper, and the intermodulation frequen-

cies are the same. The equality of the two expansions is thus proven.

This approach, although slightly more complicated conceptually, is mathematically rigorous. It takes into account all of Grayzel's objections of mathematical inconsistencies and leads to the same expansion found in (21) and (22) of the paper, thereby showing the correctness and validity of the results.

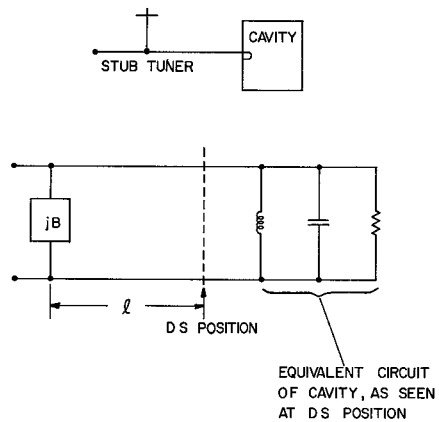


Fig. 1. Composite resonator formed by adding a shunt susceptance in the cavity feeder line.

### On Changing the Coupling into a Microwave Cavity by Means of a Stub Tuner

In microwave measurements involving a resonant cavity it is sometimes desirable to be able to make a continuous adjustment of the coupling coefficient, defined as<sup>1</sup>

$$\beta = \frac{Q_0}{Q_{\text{ext}}}. \quad (1)$$

Variation of  $Q_0$  by adjustment of the spatial distribution of loss within the cavity and variation of  $Q_{\text{ext}}$  by mechanical adjustment of the coupling loop or aperture are both often impractical, particularly in situations where it is difficult to gain access to the cavity while data are being taken. However, one can also vary the coupling coefficient by inserting a shunt susceptance (stub tuner) into the feeder line, at some distance away from the cavity. The problem of calculating the magnitude and location of this susceptance differs somewhat from the standard fixed-frequency or narrow-band matching problem,<sup>2</sup> because the impedance being "matched" has a strong and characteristic frequency dependence. The purpose of this correspondence is to consider this design problem.

By attaching the shunt susceptance, one forms in effect a new composite resonant system (Fig. 1), consisting of the shunt susceptance added to the cavity admittance, with the latter transformed by the line segment between the detuned-short (DS) position and the position of the shunt susceptance. The DS position serves as a convenient reference location because the equivalent representation of the cavity assumes the simple shunt form of Fig. 1 only when viewed from there. The  $Q$  of this composite system can in principle be calculated analytically from the known composite admittance function,<sup>3</sup> but a much simpler approach can be made by using the Smith chart.

Manuscript received June 16, 1966; revised October 16, 1966. This work was supported by the Air Force Systems Command, Rome Air Development Center, Griffiss AFB, Rome, N. Y.

<sup>1</sup> E. L. Ginzton, *Microwave Measurements*, New York: McGraw-Hill, 1957, ch. 9.

<sup>2</sup> R. E. Collin, *Foundations for Microwave Engineering*, New York: McGraw-Hill, 1966, ch. 5.

<sup>3</sup> C. G. Montgomery, R. H. Dicke, and E. M. Purcell, *Principles of Microwave Circuits*, New York: McGraw-Hill, 1948, ch. 7.

On a Smith chart a plot of the cavity impedance, observed at the DS position over a frequency range near resonance, will result in a circle through the point  $R/Z_0 = 0$ . The numerical value of  $\beta$  can then be read directly from this characteristic as the normalized resistance offered by the cavity at resonance. The diameter of the impedance diagram is thus directly related to the magnitude of the coupling coefficient  $\beta$ . Actually, for the purposes of this discussion, the cavity admittance circle (as seen at the DS position) is of greater interest; it is obtained by reflecting the impedance circle through the center of the Smith chart.

In using the Smith chart to describe the behavior of the composite system one assumes, first, that the shunt susceptance is essentially constant with frequency over the entire cavity bandwidth. This assumption is quite realistic, provided the magnitude of the shunt susceptance is kept reasonably small ( $B/Y_0 < 1$ ). Second, the transmission line segment between shunt susceptance and cavity must not have a large standing-wave field and it must be reasonably short, so that one can assume the amount of energy stored there to be negligible compared to the energy stored in the cavity. This assumption also is satisfied only for small values of shunt susceptance. As the latter is increased, the  $Q_0$  of the composite system will deviate more and more from the true  $Q_0$  of the cavity.

We will now consider the behavior of the composite system. If a shunt susceptance is added at a position which is an integral number of half-wavelengths away from the DS ( $l = (n/2)\lambda_g$ ), the cavity will simply be detuned, since one is then adding a reactive element in parallel to the equivalent resonant circuit. The size of the admittance circle remains invariant in this case, and there is no resultant change in the coupling coefficient. If, on the other hand, a shunt susceptance ( $\pm jB$ ) is added at  $DS \pm \frac{1}{4}\lambda_g$ , then the size of the circle must always decrease. This can be seen in Fig. 2, which shows the admittance circle  $y_1$  rotated through  $\frac{1}{4}\lambda_g$  to position  $y_2$ , where the shunt susceptance is then added. For example, if  $B/Y_0 = +3.0$ , the composite admittance circle then appears at  $y_3$ , and it is much smaller than  $y_1$ . Finally, from Fig. 2 it is clear that with the shunt susceptance placed near

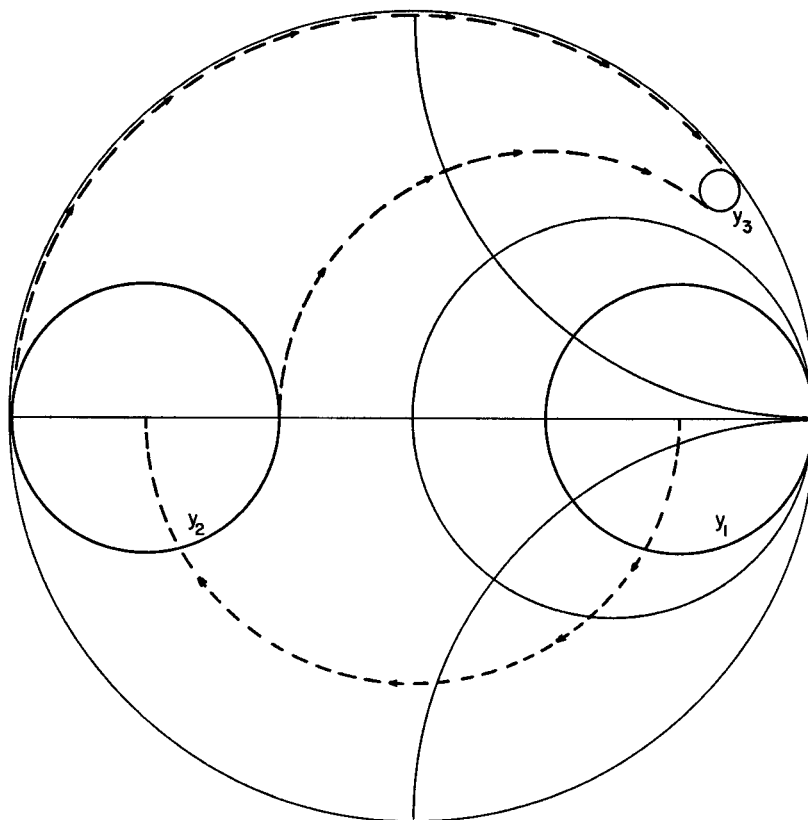


Fig. 2. Modification of Smith-chart admittance diagram by addition of shunt susceptance  $j(B/Y_0) = j3.0$  at  $DS \pm \frac{1}{2}\lambda_g$ .

$DS \pm \frac{1}{2}\lambda_g$ , the size of the circle, and hence the coupling coefficient, can be either increased or decreased, depending on the sign of the susceptance being added. The magnitude of the desired susceptance is easily obtained by fitting an admittance circle of the desired size between the appropriate constant-conductance contours, such as the dashed lines connecting  $y_2$  and  $y_3$  in Fig. 2, and observing the difference, in terms of susceptance, between the shifted admittance circle  $y_2$  and the desired admittance circle  $y_3$ .

#### EXPERIMENTAL RESULTS AND CONCLUSION

The experimental cavity consisted of a three-inch section of ring-bar slow-wave structure that was mounted between transverse shorting planes,<sup>4</sup> and that possessed a longitudinal resonance at 1090 MHz. Coupling was achieved by direct connection of the center conductor from a BNC terminal to a ring near one end of the cavity.

In order to modify the coupling to this resonant mode a single stub tuner (modified Weinschel DS 109L) was used to produce  $jB/Y_0 = j1.0$  at a position  $DS + 0.89\lambda_g$ , "towards load," i.e., the tuner was placed between the cavity and the DS position. Physically, the tuner was located within less than  $\frac{1}{2}\lambda_g$  from the cavity terminal. The results are summarized in Table I.

It is seen that by attaching the stub tuner,

<sup>4</sup> B. Kulke, "An extended-interaction klystron: efficiency and bandwidth," Microwave Lab., Stanford University, Stanford, Calif., M.L. Rept. 1320, ch. 4, May 1965.

TABLE I

Quantity	Without stub tuner	With stub tuner set to give $jB/Y_0 = j1.0$
$Q_0$	111	90
$Q_{ext}$	53	22
$Q_L$	36	18
$\beta$	2.1	4.1 measured 5.5 predicted

$Q_L$  is decreased by a factor of two. The "predicted"  $\beta = 5.5$  was obtained by graphically adding the shunt susceptance (assumed constant) to the rotated admittance circle, as was explained. This compared with a measured  $\beta = 4.1$ , with the stub tuner attached. Since both this discrepancy and the change in  $Q_0$  are somewhat greater than might be expected from measurement error, one suspects that in this case the energy stored and dissipated outside the cavity was not negligible. In subsequent measurements the setting of the stub tuner was varied to produce a wide range of values for  $Q_{ext}$ , but no further significant change was observed in  $Q_0$  ( $Q_{ext} = 49, 70, 87, 125$  with  $Q_0 = 88, 86, 87, 92$ ). The apparent change in  $Q_0$  that occurred when the stub tuner was first inserted into the feeder line, was, therefore, probably due to residual reflections from the tuner or its type *N* connectors, rather than to excessive tuner susceptance as one would at first expect. Clearly, the method does afford a quick and simple way of changing the cavity loading, provided that the shunt susceptance (including residual reflections) is limited to reasonably small values.

#### LIST OF SYMBOLS

$\beta$  coupling coefficient.  
 $Q_0, Q_{ext}, Q_L$  internal, external, and loaded  $Q$ .  
 DS detuned-short.  
 $Z_0, Y_0$  characteristic impedance, admittance of feeder line.  
 $B$  shunt susceptance.  
 $l$  distance between DS and shunt susceptance.  
 $\lambda_g$  guide wavelength in feeder line.

#### ACKNOWLEDGMENT

The author is indebted to Prof. M. Chodorow, of Stanford University, Stanford, Calif., for several stimulating discussions.

BERNHARD KULKE  
 Dept. of Elec. Engrg.  
 Syracuse University  
 Syracuse, N. Y.

#### The Point-Matching Method for Interior and Exterior Two-Dimensional Boundary Value Problems

There have appeared recently some papers [1]–[4] on a "point-matching method" for solving electromagnetic boundary value problems. The only attempts at justifying its use have been qualitative, but the method is plausible, and in some instances gives accurate results. Nevertheless, the method is unsound, in general, as has been pointed out by Harrington [5]. It will be demonstrated, however, that when certain symmetries are maintained, the point-matching method is valid. These symmetries are maintained, or nearly maintained, in the majority of test cases used for "demonstrating" the validity of the method, which explains its apparent success.<sup>1</sup> Yee [6] and Laura [7], [8] describe the background of the method and the motivation for its use.

A single type of electromagnetic boundary value problem will be considered: an infinite, perfectly conducting, cylindrical boundary of arbitrary cross section with the (monochromatic) electric field parallel to the axis of the cylindrical boundary. This type of problem is adequate both for explaining the successes of the point-matching method in special cases and for displaying its inadequacy in general. Figure 1 shows an infinite cylindrical boundary  $C$ , supposed perfectly conducting, described by the cylindrical polar coordinates  $r$  and  $\theta$ . The point  $P$  at which the field is observed is described by the cylindrical polar coordinates  $\rho$  and  $\phi$ . The electric field is constrained to be perpendicular to the paper so that the fields are most conveniently represented by the component of the vector poten-

Manuscript received July 5, 1966; revised October 3, 1966.

<sup>1</sup> It is interesting that these symmetries are maintained in all of the actual calculations quoted by Yee and Audeh [13] in a recent paper.